論文の内容の要旨

論文題目　バイオインフォマティクスによる H5N1 トリインフルエンザウイルス感染の解析

氏　　名　高野　量

Chapter I. Molecular mechanisms underlying oseltamivir resistance mediated by an I117V substitution in the NA of H5N1 avian influenza viruses.

The neuraminidase (NA) inhibitors oseltamivir and zanamivir are widely used to treat patients infected with influenza viruses. An Ile-to-Val change at position 117 in NA (NA-I117V), found in some H5N1 highly pathogenic viruses isolated from humans and birds, confers limited resistance to oseltamivir carboxylate *in vitro*. To evaluate the effect of this NA-I117V mutation on the efficacy of oseltamivir, we created single point mutant viruses with three genetically different backgrounds. Although the NA-I117V substitution did not substantially affect NA enzymatic activity, it conferred slight resistance to oseltamivir *in vitro* (1.3- to 6.3-fold changes). Mice infected with I117V virus exhibited reduced susceptibility to oseltamivir and decreased survival in two of three virus pairs tested. Molecular dynamics simulations revealed that although the amino acid at position 117 of NA did not directly interact with oseltamivir carboxylate, the NA-I117V substitution caused the loss of hydrogen bonds between an arginine at position 118 (R118) and the carboxyl group of oseltamivir (Fig. 1). This distortion could have caused the slightly lower binding affinity for oseltamivir compared to wild-type NA. Viruses that possess the NA-I117V substitution are found mostly in avian isolates, suggesting that viruses with reduced susceptibility to oseltamivir emerged spontaneously. Our findings provide new insights into the mechanism of NA-I117V-mediated oseltamivir resistance, which should be of value to those who select antiviral drug regimens for patients infected with H5N1 viruses.

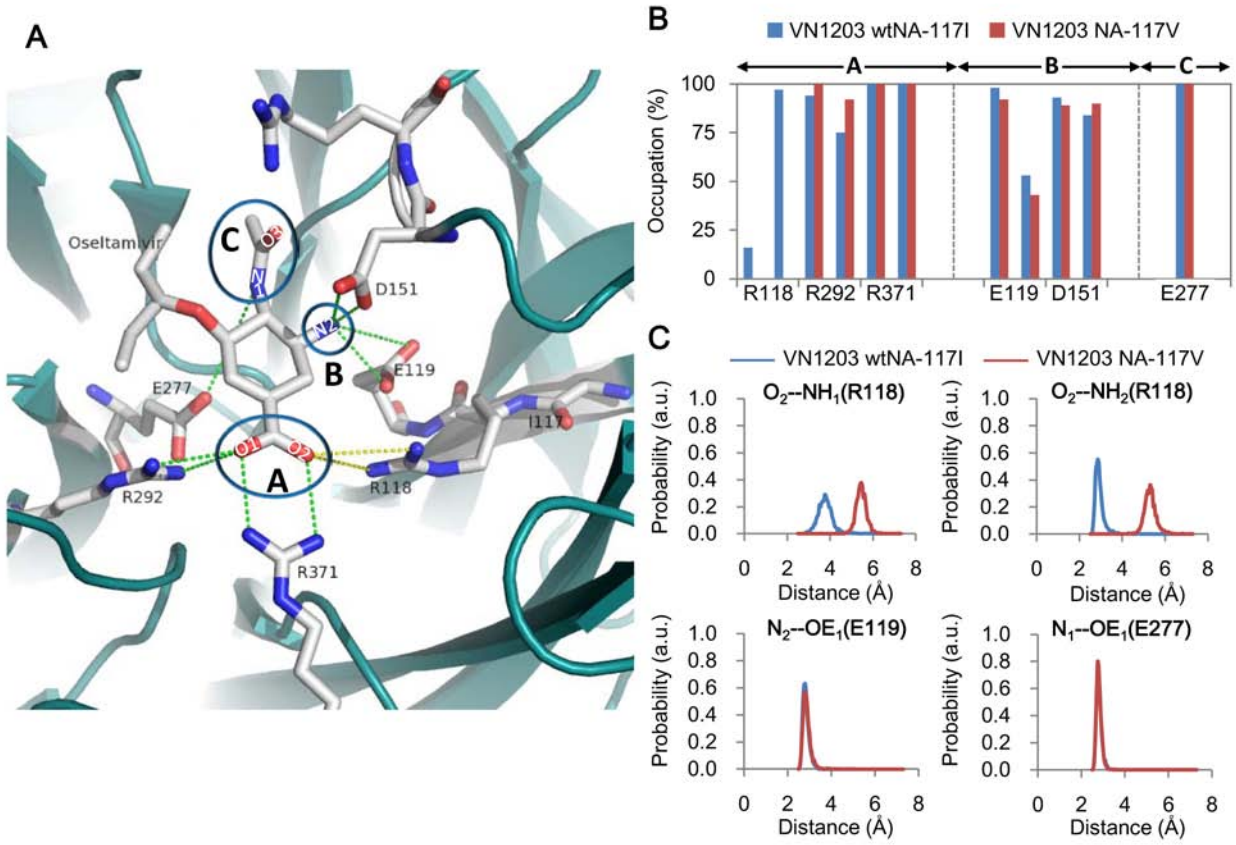

Figure 1. Hydrogen bonds between residues in the binding pocket of neuraminidase and oseltamivir predicted by using molecular dynamics simulations. (A) Amino acid residues analyzed for hydrogen bonding are shown in the structure of the N1 neuraminidase in complex with oseltamivir. (B) Percent occupation pattern of hydrogen bonds between residues of oseltamivir and neuraminidase for wild-type and I117V NA. (C) Inter-atomic distances of hydrogen bonds between oseltamivir and residues R118, E119, and E277 of neuraminidase.

Chapter II. Determinants of mice survival/death in H5N1 virus infections.

"Hypercytokinemia" and the "cytokine storm", which are characterized by the elevated expression of proinflammatory cytokines, are thought to be the main cause of death in human infection with H5N1 viruses. The mouse is widely used for studying viral pathogenesis of H5N1 avian influenza virus. Mice infected with H5N1 viruses produce lethal pneumonia with systemic virus infection; however, the determinants of mice survival/death in H5N1 virus infections remain poorly understood. Viral pathogenicity in mice is usually determined on the basis of the 50% of mouse lethal dose (MLD50); however, we found an H5N1 virus strain, isolated in Indonesia in 2007, that shows virus-dose-independent

lethality in mice (Fig. 2). Mice infected with this virus at 10^7 plaque-forming units (PFU) showed severe clinical signs with marked weight loss, but 75% of them survived. By contrast, 80% of mice died following infection with a lower dose of the virus (10^5 PFU). By revealing the mechanism of recovery of mice infected with this virus at high dose, we could provide new insights into the pathogenicity of H5N1 viruses.

To investigate how the initial dose of virus inoculum influences H5N1 virus infections, we first investigated the virus titers in multiple tissue organs. The initial dose of virus inoculum determined the virus growth kinetics in the respiratory tracts and the extent of virus dissemination in the spleens and brains of mice (Fig. 3). Of note, a higher virus inoculum was not better for virus replication in the lungs or for virus dissemination into multiple organs. Next, to clarify the difference in host immune responses in mice infected with H5N1 viruses at various doses, we analyzed the expression levels of 32 cytokines in the lungs of mice. The cytokine/chemokine expression array analyses revealed that "hypercytokinemia" and a "cytokine storm" are not directly responsible for the death of mice infected with H5N1 viruses at a lower infection dose (10^5 PFU). To clarify the different host responses in the lungs of mice infected with H5N1 viruses at the gene transcriptional level, we performed oligonucleotide-based DNA microarrays. Global gene transcriptional analysis identified gene networks that were strongly correlated with the virus growth kinetics in mouse lungs and could be responsible for the severity of the high-dose infection in mice that results in death. Integrated global and dynamic host responses thus highlight the molecular gene networks that are strongly associated with the amount of virus that is present in the lungs, which, in turn, could determine whether or not a mouse survives an H5N1 virus infection.

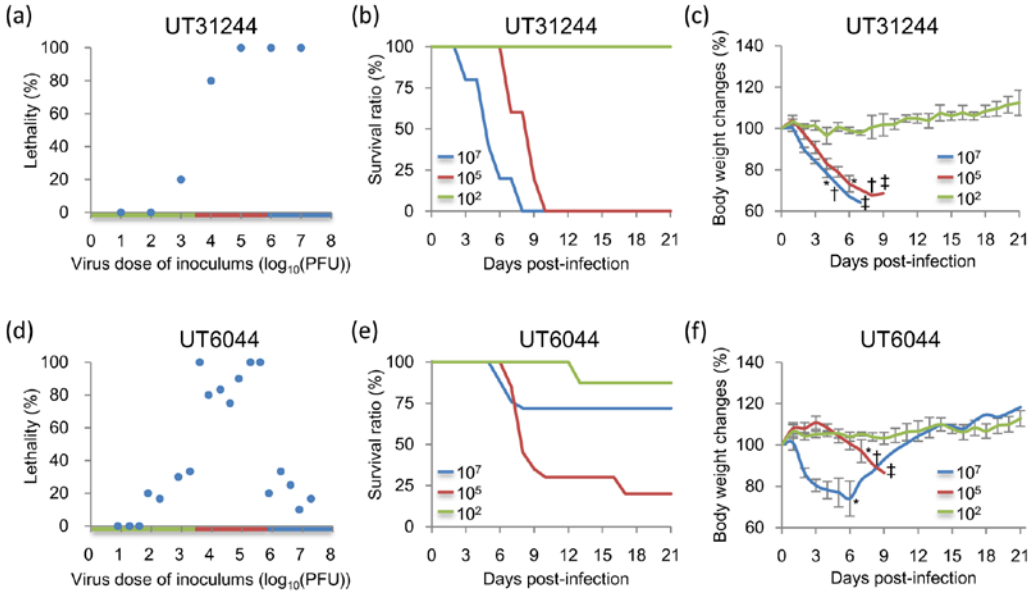

Figure 2. Lethality of two H5N1 viruses in mice. Mice were intranasally infected with viruses from serial dilutions of viruses that ranged from 10^1 to 10^8 PFU. Mouse mortality was observed daily for 21 dpi for UT31244 (a) and UT6044 (d) virus infections. Percent survival and body weight are shown for each group of three mice infected with UT31244 (b, c) and UT6044 (e, f) viruses at 10^2, 10^5, and 10^7 PFU, respectively.

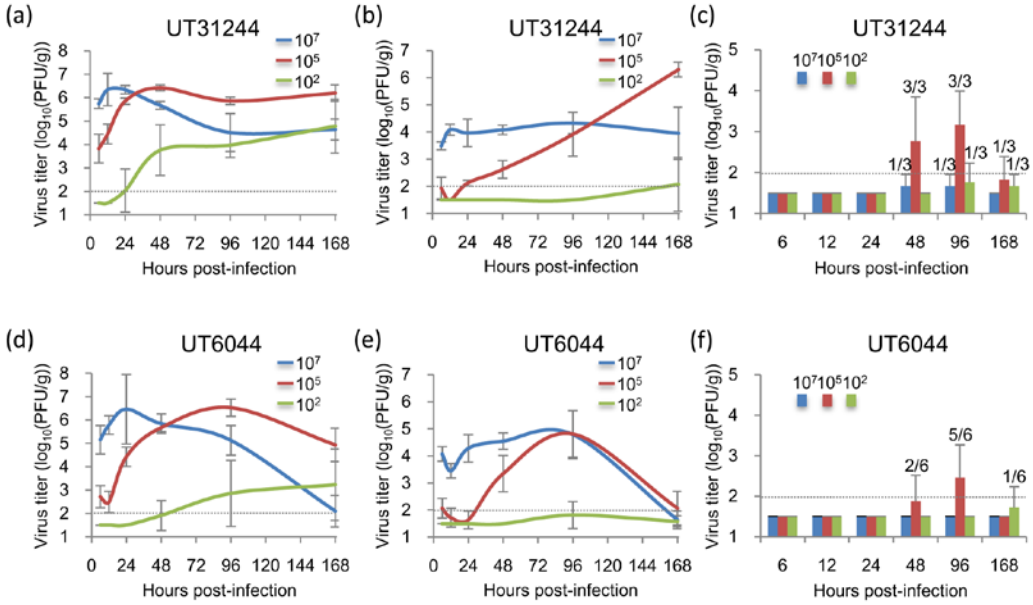

Figure 3. Virus growth kinetics in respiratory tracts and solid organs in mice. Mice were intranasally infected with viruses at 10^2, 10^5, and 10^7 PFU; three and six mice in the UT31244 and UT6044 groups, respectively, were euthanized on hours 6, 12, 24, 48, 96, and 168 pi. Lungs (a, d), nasal turbinates (b, e), and spleens (c, f) were collected at each time point, and virus in tissues was titrated by using plaque assays in MDCK cells. (c, f) The number above the bar graph indicated the number of mice from whose spleens virus was detected relative to the total number of mice. The detection limit of virus titer was < 2.0 $\log_{10}$(PFU/g). For the downstream analyses, the value below the detection limit was set as 1.5 $\log_{10}$(PFU/g).